Solar Energy Materials and Solar Cells 175 (2018) 29–34

Contents lists available at ScienceDirect

Solar Energy Materials and Solar Cells

journal homepage: www.elsevier.com/locate/solmat

Enhancing the efficiency of transparent dye-sensitized solar cells using concentrated light

Prabhakaran Selvaraj[a,*], Hasan Baig[a], Tapas K. Mallick[a], Jonathan Siviter[b], Andrea Montecucco[b], Wen Li[b], Manosh Paul[b], Tracy Sweet[c], Min Gao[c], Andrew R. Knox[b], Senthilarasu Sundaram[a,*]

[a] Environment and Sustainability Institute (ESI), University of Exeter, Penryn Campus, TR10 9FE, United Kingdom
[b] School of Engineering, University of Glasgow, Glasgow G12 8QQ, United Kingdom
[c] School of Engineering, Cardiff University, Cardiff CF24 3AA, United Kingdom

ARTICLE INFO

Keywords:
Dye-sensitized solar cell (DSSC)
Low Concentrating Photovoltaics (LCPV)
Temperature effect on DSSC
Scale up of DSSC

ABSTRACT

Transparent dye-sensitized solar cells (DSSCs) can be coupled within a building's architecture to provide daylighting and electrical power simultaneously. In this work, the relationship between the transparency and performance of DSSCs is studied by changing the TiO_2 electrode thickness. The 10 μm thickness device shows a power conversion efficiency of 5.93% and a J_{sc} of 12.75 mA/cm^2 with 37% transparency in the visible range. However, the performance loss in DSSCs during the scale up process is a potential drawback. This can be addressed using an optical concentrator with DSSC to generate more power from small size devices. Here, a compound parabolic concentrator (CPC) is coupled with DSSCs and its performance is compared to a scaled-up device (approx. 4 times). Furthermore, the impact of operating temperature on the performance of the bare and concentrator-coupled devices is discussed in this article. An increase of 67% in power conversion efficiency is observed at 36 °C for the concentrator-coupled device under 1000 W/m^2 illumination. Maximum J_{sc} of 25.55 mA/cm^2 is achieved at 40 °C for the concentrated coupled device compare with the J_{sc} of 13.06 mA/cm^2 for the bare cell at the same temperature.

1. Introduction

Dye-sensitized solar cells (DSSCs) have gained much attention in recent years [1,2] due to their simple manufacturing process, low cost of materials, light weight, flexibility, good photocurrent conversion efficiency, short energy payback time and tunable optical properties [3–5]. Even though DSSCs have achieved PCEs over 14% [3,6] with small active area, the power output decreases with an increase in the cell active area of the photoanode [7]. This is due to some unfavourable issues such as non-homogeneous and non-uniform titania layers because of large area deposition, dye sensitisation and electrolyte filling issues also electrical interconnection of individual cells [8]. However, the performance loss during scale up can be addressed by coupling optical concentrators with small DSSC. Concentrating Photovoltaic (CPV) systems make use of optical components which concentrate the incoming sunlight and focus it on solar cells. The concentrated light reaching the solar cell increases the energy production several times [9–11]. Based on the light illumination intensity it focuses on the solar cell, the concentrators may be classified as low concentration systems, medium concentration systems and high concentrator systems. Low concentration systems are usually simple in their design, manufacture and operation. These systems have a concentration factor of less than 10× [12]. Due to its versatility in applications and geometries, a type of low concentrator – the compound parabolic concentrator (CPC) is used in low and medium temperature ranges [13].

The application of an optical lens-based solar concentrator system mounted on top of DSSCs still poses several challenges in terms of efficiency, cost-effectiveness of optical design, and the provision of uniform and concentrated illumination on a DSSC [14]. Furthermore, various complex phenomena including light scattering, recombination of electron-hole pairs, and dye degradation in the photoactive layers of DSSCs can occur when the intensity of incident light is increased by a solar concentrator [15]. A considerable amount of research has been conducted on increasing the electrical efficiency of DSSCs and their modules [16–18]. Moon et al. [19] employed concentrated illumination using a condenser lens up to 3.72 suns on a DSSC and it was found that an increase in photocurrent and efficiency values. Choi et al. [20] used condenser lens for a vertical stacked- cell configuration DSSC in to increase the efficiency and at 8 mm separation distance between the lens and the cell, the device efficiency increased from 2.5% to 8.3%. Barber

* Corresponding authors.
E-mail addresses: ps364@exeter.ac.uk (P. Selvaraj), S.Sundaram@exeter.ac.uk (S. Sundaram).

http://dx.doi.org/10.1016/j.solmat.2017.10.006
Received 20 July 2017; Received in revised form 4 September 2017; Accepted 9 October 2017

et al. [21] proposed a concentrator for a hybrid silicon-DSSC system with two different optical filters for visible and IR absorption to achieve about 20% efficiency. More recently, Sacco et al. [22] demonstrated the application of a solar concentrator both in indoor and outdoor working conditions. The outdoor results show a linear behaviour for solar concentration factors up to 1.5. However, the LCPV has not been used on DSSC before. This article focuses on the performance of transparent DSSCs under low concentrated light.

In this work, we report the optical and electrical performance of transparent DSSCs by changing the working electrode thicknesses. A Low concentrator with 3× optical concentration was designed and employed to study the effect of light concentration on DSSCs. Moreover, a systematic study of the temperature dependency on the performance of bare DSSCs and those coupled with LCPV system has been carried out.

2. Experimental methods

2.1. DSSC fabrication

The working electrodes and the corresponding devices were prepared according to the literature procedures [23]. Fluorine doped transparent conducting SnO_2 (FTO) glass substrates (Pilkington 2.2 mm, 13 Ω/sq) were cleaned with distilled water and ethanol. A layer of 20 nm transparent TiO_2 paste (Dyesol 18NR-T) was coated on the conductive glass by screen printing. This was repeated (2–7 layers) to obtain different thicknesses for the working electrode (Labelled as devices L2-L7). The thickness of the TiO_2 electrodes was measured using Dektak 8 Advanced Development Profiler. In order to remove the organic particles, prepared thin films were annealed rapidly at 450 °C for 30 min. After cooling them to 80 °C, the TiO_2 electrodes were immersed into 0.2 mM N719 dye in ethanol at room temperature for 12–15 h. The iodide/tri-iodide electrolyte comprising 0.4 M LiI, 0.4 M tetrabutylammonium iodide (TBAI), and 0.04 M I_2 dissolved in 0.3 M N-methylbenzimidazole (NMB) in acetonitrile (ACN) and 3-methoxypropionitrile (MPN) solvent mixture at a volume ratio of 1:1 was prepared and stirred for 24 h at room temperature [24]. Pt electrode was placed over the dye-adsorbed TiO_2 electrode with a 25 μm hot-melt spacer between two electrodes. Iodide/tri-iodide electrolyte was introduced into the cell through the small hole drilled in the counter electrode. The active area of the TiO_2 electrodes was 0.28 cm^2. The hole in the counter electrode was sealed with a film (Meltonix- Solaronix) and a piece of cover glass. The transparency of the bare devices was measured using a UV–VIS–NIR spectrometer (PerkinElmer, Lambda 1050).

2.2. Low concentrator fabrication

Fig. 1 shows the fabrication of the concentrator with a geometrical concentration factor of C = 4×. The concentrator was printed into two halves (Fig. 1**(a)**), reflective film (94%) was adhered on the CPC surface (Fig. 1**(b)**), and the two halves were assembled together as shown in (Fig. 1**(c)**). The concentrator was placed on top of the solar cell for testing. (Fig. 1**(d)**)

2.3. Device characterization

In an indoor controlled environment, the CPV unit was tested to evaluate the impact of radiation intensity. The setup essentially consists of a solar simulator which is a light source from a xenon lamp emanating collimated light rays and an I-V tracer which is used to characterise the electrical performance of the solar cell. The photovoltaic performances of the assembled devices were measured under 1000 W/m^2 of light from a Wacom AAA continuous solar simulator (model: WXS-210S-20, AM1.5G). The I–V characteristics of the devices was recorded using EKO MP-160i I–V Tracer (similar set up used previously)

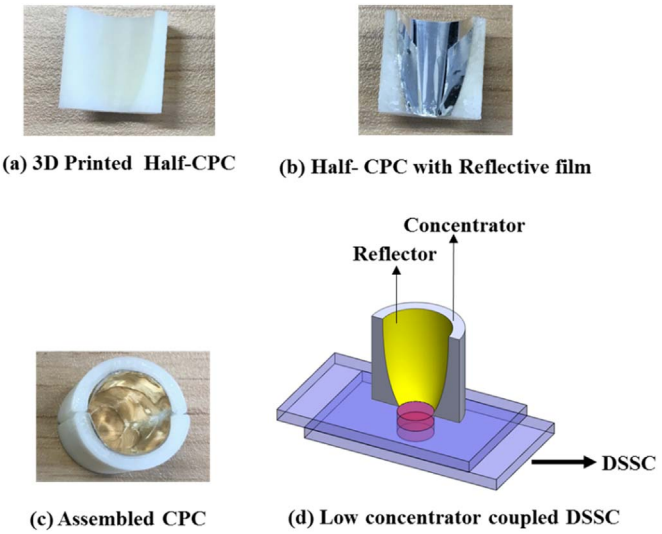

Fig. 1. Fabricated low concentrator. (a) one half of the printed concentrator, (b) adhered reflective film, (c) assembled concentrator used for this work and, (d) low concentrator coupled DSSC.

[25]. The temperature of the devices was recorded using an OMEGA RDXL 12SD temperature recorder. Finally, the concentrator unit was placed on the DSSC to perform DSSC-LCPV measurements.

3. Results and discussion

The advantage of making transparent DSSCs is easily adopt them into building architectures. So, the degree of transparency of DSSCs should be carefully taken into account when evaluating the efficiency of DSSCs [26]. The transparency of DSSCs is heavily depending on the thickness of TiO_2 nanostructured materials. Fig. 2. shows **(a)** the relationship between TiO_2 thickness and DSSC device transparency, and **(b)** current density-voltage (J-V) curves of the corresponding devices. The average transparency of 53% was recorded for the device made with 3.5 μm thick TiO_2 electrode (L2) and the device with 14 μm thick TiO_2 electrode has 19% transparency. When the TiO_2 layer thickness was increased from 3.5 to 10 μm an obvious increase of J_{sc} from 7.36 mA/cm^2 to 12.75 mA/cm^2 was occurred in the corresponding devices, resulting in a corresponding improvement of efficiency from 2.51% to 5.93%. More dye molecules attached to the thick TiO_2 films absorb more light, leading to low transmittance, also thick films physically block/absorb the light [26]. Conversely, the photovoltaic performance decreased after 10 μm thick TiO_2 with further increase in titania layer thickness (12 μm, 14 μm) [27–29]. This is due to increase the length of the electron pathways, and thus decrease FF and V_{oc} [30–32]. The photovoltaic parameters of the devices with different TiO_2 thickness are given in Table 1.

3.1. Scaled up device- comparison with LCPV coupled device

In order to use DSSCs as building integrated photovoltaic (BIPV) element, the devices need to be prepared as transparent as possible especially for window applications. Due to this, scaling up of DSSC has become an important process even though it has associated with different issues. Here, 1.1 cm^2 active area DSSC device with 10 μm titania thickness and 37% transparency was fabricated to study the performance of a scale-up device (Fig. 3). Fig. 4**(a), (b)** shows the current density -voltage and power density – voltage behaviour respectively for device with an active area of 0.28 cm^2 and 1.1 cm^2 (~ 4 times larger area than 0.28 cm^2). The short circuit current of 1.1 cm^2 active area device is higher than the small area device. However, the current density and power density of the scaled up DSSC is much lower than the

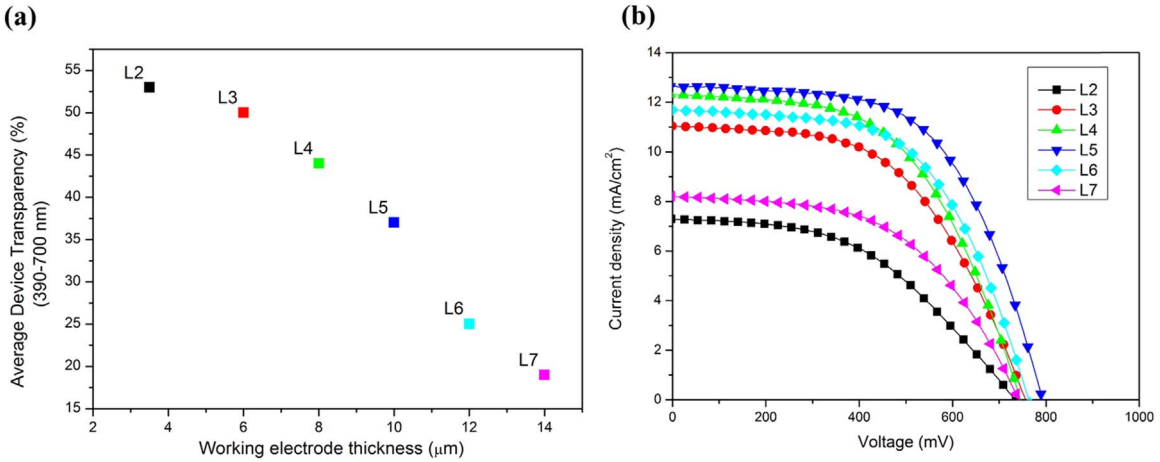

Fig. 2. (a) Effect of working electrode thickness on device transparency, **(b)** Photocurrent density-voltage (J-V) curves of the bare DSSCs based on different TiO_2 thicknesses.

Table 1
Photovoltaic parameters of the bare cells based on different TiO_2 thicknesses under an illumination of 1000 W/m^2 (AM 1.5G).

Device	TiO_2 thickness (μm)	J_{sc} [mA/cm^2]	V_{oc} [mV]	ff [%]	P_{max} [mW/cm^2]	η [%]
L2	3.5	7.36	733	46.6	2.48	2.51
L3	6.0	11.14	756	54.0	4.46	4.49
L4	8.0	12.42	746	56.2	4.99	5.02
L5	10.0	12.75	793	58.7	5.87	5.93
L6	12.0	11.81	763	59.0	5.10	5.15
L7	14.0	8.28	742	56.6	3.22	3.24

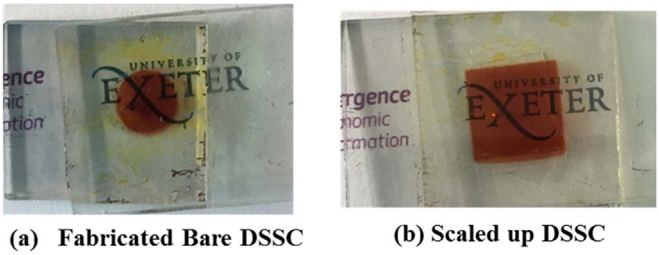

Fig. 3. Fabricated L5 devices. (a) Small active area bare DSSC and (b) Scaled-up device.

Table 2
Photocurrent density – voltage (J-V) parameters of the bare cells and scaled up device under an illumination of 1000 W/m^2 (AM 1.5G).

Device	I_{sc} [mA]	J_{sc} [mA/cm^2]	V_{oc} [mV]	ff [%]	P_{max} [mW/ cm^2]	η [%]
L5	3.60	12.75	793	58.7	5.87	5.93
L5–1.1 cm^2	7.76	6.93	773	49.3	2.96	2.64

small area devices. Due to the high sheet resistance, which causes Ohmic loss and further leads to a significantly reduced fill-factor as well as efficiency of the scaled-up devices [33]. (Table 2).

3.2. Low concentrator coupled devices

The LCPV system was placed on DSSCs to understand the photovoltaic performance of DSSCs under concentrated light. Fig. 5 and Table 3 show the photocurrent density-voltage characteristics and the photovoltaic parameters of the DSSCs coupled with the low concentrator system. It is clear from the table that J_{sc} of the devices coupled with the concentrator increased with the TiO_2 electrode thickness. Device L5C has the highest J_{sc} of 23.16 mA/cm^2, which is 82% higher than the corresponding bare device. Increase in the short circuit current is due to the concentrated light. Like silicon solar cells, open circuit

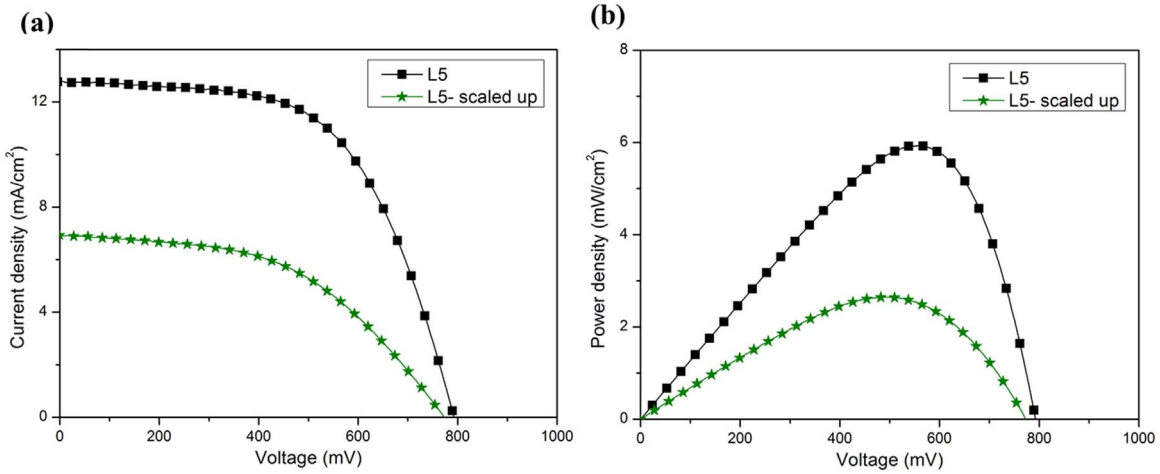

Fig. 4. Comparison of **(a)** J-V curves, and **(b)** power density of the small area bare cells, coupled with LCPV and scaled up device.

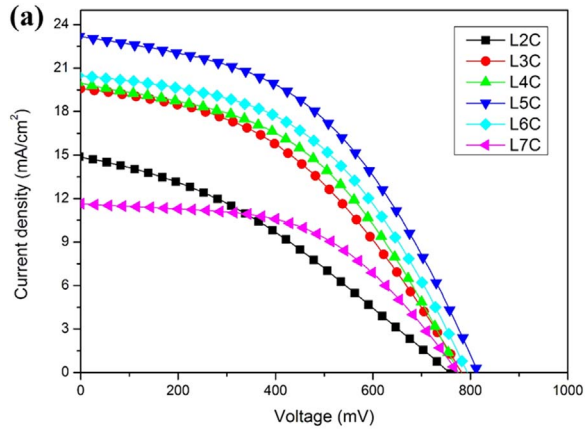

Fig. 5. Photocurrent density-voltage (J-V) curves for the low concentrator coupled devices based on different TiO_2 thicknesses.

Table 3
Photovoltaic parameters of the cells based on different TiO_2 thicknesses with low concentrator under an illumination of 1000 W/m^2 (AM 1.5G).

Device	J_{sc} [mA/cm^2]	V_{oc} [mV]	ff [%]	P_{max} [mW/ cm^2]	η [%]
L2C	14.86	757	34.4	3.89	3.90
L3C	19.55	782	42.7	6.55	6.60
L4C	19.96	775	45.6	7.08	7.12
L5C	23.16	816	46.2	8.74	8.82
L6C	20.48	794	47.3	7.68	7.77
L7C	11.63	774	53.5	4.63	4.69

voltage of DSSC increases logarithmically with light intensity according to the equation below,

$$V'_{oc} = V_{oc} + \frac{nkT}{q} \ln X$$

where X is the concentration of sunlight [34].

Although fill factor decreased for all the devices compared with the bare cells, which could be due to more electron recombination, but the overall photovoltaic performance increased for all the devices coupled with the low concentrator.

The photovoltaic performances of bare and concentrator coupled DSSCs with respect to TiO_2 film thickness are compared in Fig. 6**(a)-(d)**. It is clear that the concentrator coupled devices perform better than their bare counterparts. From the comparison, device L5 with 10 μm TiO_2 thickness is found to be the best of all devices with 5.9% and 8.8% PCE for bare and concentrator coupled cells respectively. To find the concentrator intensity output, a 0.28 cm^2 silicon solar cell was coupled with the same low concentrator and its performance was compared with the bare silicon solar cell. It was found that the LCPV system coupled silicon solar cell showed an optical concentration of 3.05× (Supporting information). From the comparison between L5 scaled-up device and low concentrator coupled one, the concentrator coupled device has slightly lesser current value due to the losses in reflective film. On the other hand, the current density of the concentrator coupled device is much higher than the scaled-up device which increases the overall performance. From the above comparison L5 has been found as the champion device. Therefore, device L5 has been taken for further analysis.

3.3. Impact of operating temperature

DSSC performance is very sensitive to its operating temperature, as the concentrated sunlight generates high temperature due to high light

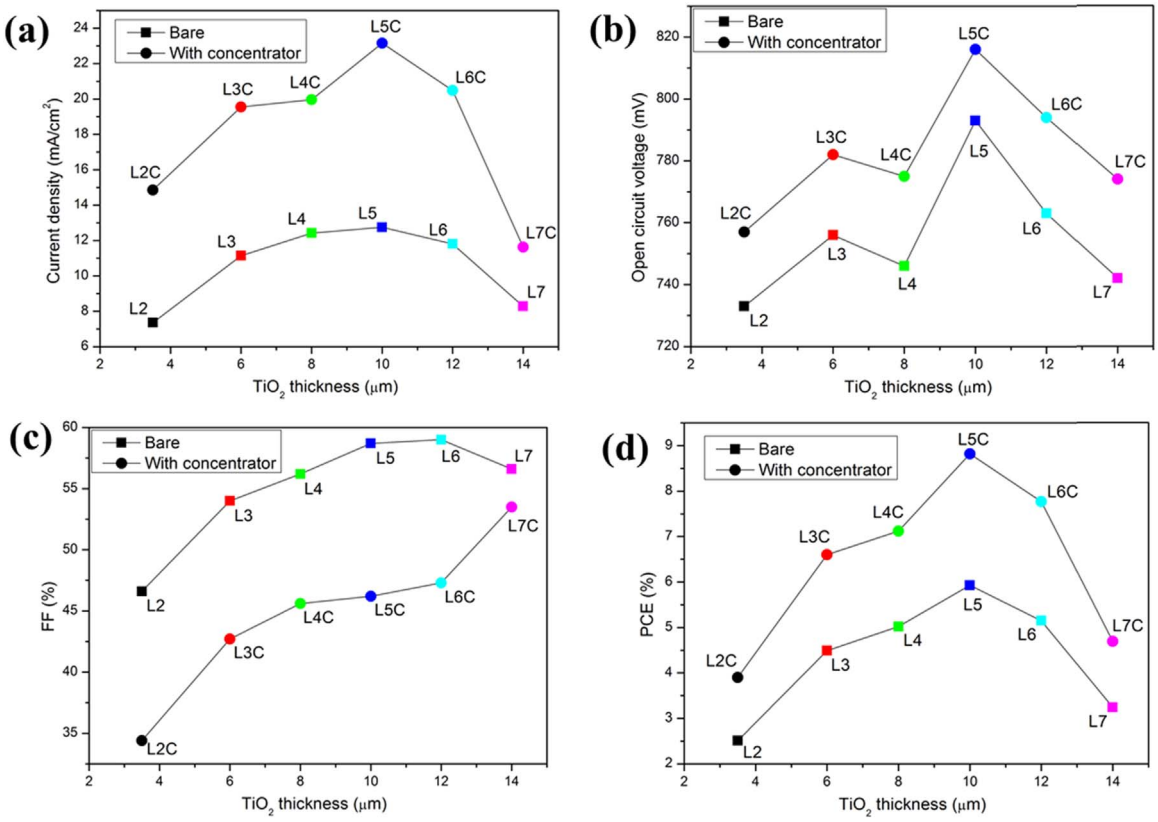

Fig. 6. Comparison of performance parameters with different working electrode thickness for bare and low concentrator coupled devices.

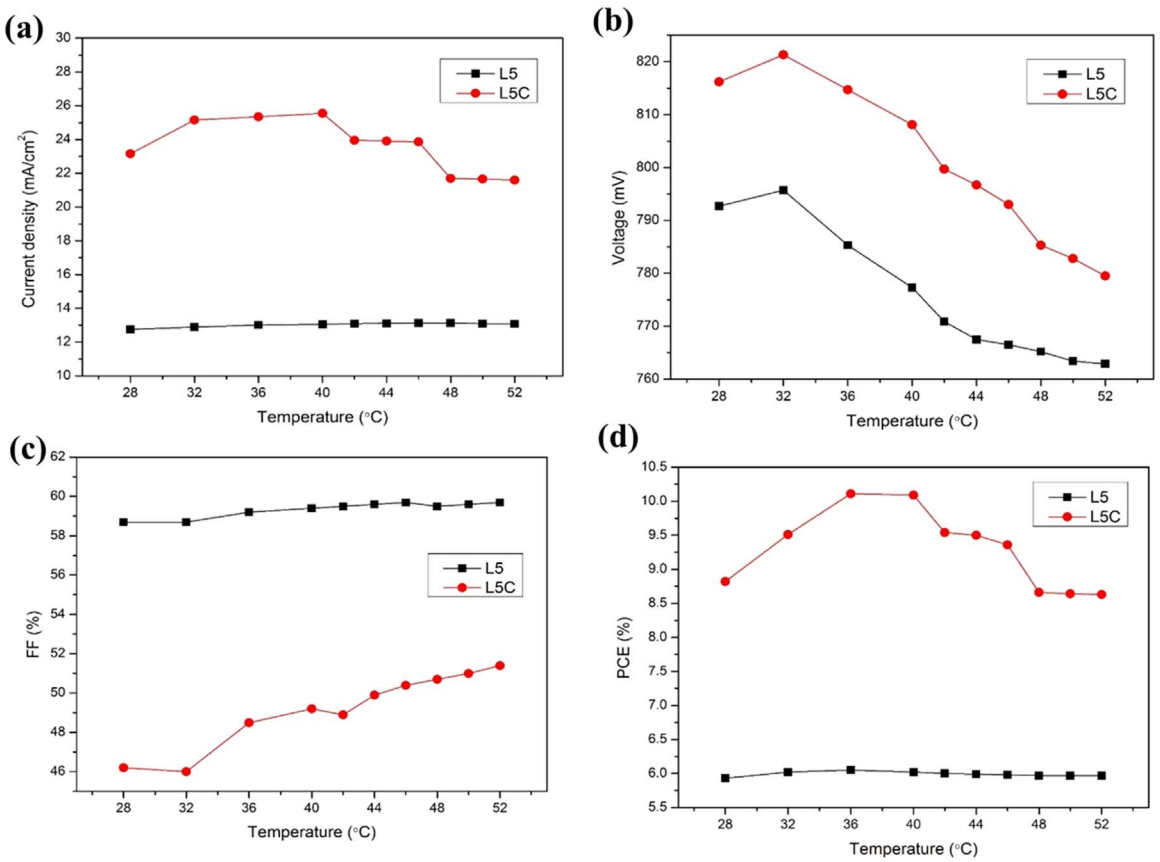

Fig. 7. Temperature dependence of the DSSC parameters of bare cell (L5) and coupled with LCPV (L5C) measured under an illumination of 1000 W/m^2 (AM 1.5G). **(a)** Temperature (°C) vs Current density (mA/cm^2), **(b)** Temperature (°C) vs Open circuit voltage (mV), **(c)** Temperature (°C) vs Fill factor, **(d)** Temperature (°C) vs power conversion efficiency.

intensity [35]. To understand the stability and behaviour of transparent DSSCs at different operating temperatures, the best performing device (L5) was tested with and without LCPV under 1 sun illumination for 20 min. It can be seen from Fig. 7**(a)** that current density (J_{sc}) for the bare device increases gradually up to 42 °C and then starts decreasing. For the device coupled with LCPV, J_{sc} increases till 40 °C and then falls, whereas, V_{oc} increases at the start then steadily decreases with temperature for both devices (Fig. 7**(b)**). On the other hand, power density reaches its maximum value at 36 °C then starts decreasing from 5.99 to 5.91 mW/cm^2 for bare devices and from 10.01 to 8.57 mW/cm^2 for low concentrator coupled devices. The maximum power conversion efficiency is recorded at 36 °C (Fig. 7**(d)**) for both the devices. It was found that the devices reached a steady state temperature of 52 °C after 20 min. Both devices show positive and negative temperature co-efficient as the power conversion efficiency of both the devices increasing till 36 °C then start decreasing. This oscillatory behaviour of the opto-electronic properties may be attributed due to the different velocities of the redox processes occurring at the TiO_2/dye, dye/electrolyte and the electrolyte/counter electrode interfaces of the DSSCs [36,37].

A low concentrator with 3× optical concentration was designed and employed on the devices, and the relationship between the transparency and performance of the devices has been understood. Due to high light intensity, the LCPV coupled devices obtained higher current density than the bare devices. Due to this, the overall performance of the solar cells increases even at high temperatures. As liquid electrolyte based DSSCs have concerns of solvent leakage and corrosion problems in the long-term process, coupling concentrators with solid state DSSCs is an option. Moreover, porphyrin sensitizers could be used to achieve high photovoltaic performance devices. Nevertheless, the energy pay-back time of DSSCs is much lower compared with silicon solar cells [38], and the low concentrators can be fabricated with low cost materials. Therefore, this system can be economically compatible with common Si solar cell based systems.

4. Conclusion

The performance of the DSSCs with various TiO_2 electrode thicknesses and transparencies was analyzed. It has been found that the photovoltaic performance of the devices increase with the thickness of the mesoporous TiO_2, before it starts decreasing for high thickness devices, which is due to long electron diffusion length. In an indoor environment, the performance of transparent DSSCs coupled with low concentrator photovoltaic system was studied. The results show that the overall performance of the LCPV system coupled devices is more than 50% higher than the bare DSSCs. To estimate the impact of operating temperature of the devices due to the addition of 3× concentrating light, the devices were measured under different temperatures for both bare and concentrator coupled cells. The results obtained demonstrate that the LCPV system coupled device stability is similar to the bare device. All the above findings will offer useful insights into solve the scaling up problem of DSSCs using solar concentrators for efficient and environmentally friendly solar cells.

Acknowledgement

The authors gratefully acknowledge financial support received from the EPSRC through Solar Challenge project SUNTRAP (EP/K022156/1).

Prof. Hari Upadhyaya and Dr. Prabhakararao Bobili, Brunel University, London for thickness measurements.

Appendix A. Supplementary material

Supplementary data associated with this article can be found in the online version at http://dx.doi.org/10.1016/j.solmat.2017.10.006.

References

[1] M. Law, L.E. Greene, J.C. Johnson, R. Saykally, P. Yang, Nanowire dye-sensitized solar cells, Nat. Mater. 4 (2005) 455–459, http://dx.doi.org/10.1038/nmat1387.

[2] D. Joly, L. Pellejà, S. Narbey, F. Oswald, J. Chiron, J.N. Clifford, E. Palomares, R. Demadrille, A robust organic dye for dye sensitized solar cells based on iodine/iodide electrolytes combining high efficiency and outstanding stability, Sci. Rep. 4 (2014) 4033, http://dx.doi.org/10.1038/srep04033.

[3] K. Kakiage, Y. Aoyama, T. Yano, K. Oya, J. Fujisawa, M. Hanaya, Highly-efficient dye-sensitized solar cells with collaborative sensitization by silyl-anchor and carboxy-anchor dyes, Chem. Commun. 51 (2015) 15894–15897, http://dx.doi.org/10.1039/C5CC06759F.

[4] S. Mathew, A. Yella, P. Gao, R. Humphry-Baker, B.F.E. Curchod, N. Ashari-Astani, I. Tavernelli, U. Rothlisberger, M.K. Nazeeruddin, M. Grätzel, Dye-sensitized solar cells with 13% efficiency achieved through the molecular engineering of porphyrin sensitizers, Nat. Chem. 6 (2014) 242–247, http://dx.doi.org/10.1038/nchem.1861.

[5] D. Joly, L. Pellejà, S. Narbey, F. Oswald, J. Chiron, J.N. Clifford, E. Palomares, R. Demadrille, A robust organic dye for dye sensitized solar cells based on iodine/iodide electrolytes combining high efficiency and outstanding stability, Sci. Rep. 4 (2014) 4033, http://dx.doi.org/10.1038/srep04033.

[6] H.M. Upadhyaya, S. Senthilarasu, M. Hsu, D.K. Kumar, solar energy materials & solar cells Recent progress and the status of dye-sensitised solar cell (DSSC) technology with state-of-the-art conversion efficiencies, Sol. Energy Mater. Sol. Cells 119 (2013) 291–295, http://dx.doi.org/10.1016/j.solmat.2013.08.031.

[7] W.J. Lee, E. Ramasamy, D.Y. Lee, J.S. Song, Dye-sensitized solar cells: scale up and current-voltage characterization, Sol. Energy Mater. Sol. Cells 91 (2007) 1676–1680, http://dx.doi.org/10.1016/j.solmat.2007.05.022.

[8] E. Stathatos, Dye sensitized solar cells: a new prospective to the solar to electrical energy conversion. issues to be solved for efficient energy harvesting, Eng. Sci. Technol. Rev. 5 (2012) 9–13.

[9] H. Apostoleris, M. Stefancich, M. Chiesa, Tracking-integrated systems for concentrating photovoltaics, Nat. Energy 1 (2016) 16018, http://dx.doi.org/10.1038/nenergy.2016.18.

[10] H. Baig, N. Sarmah, D. Chemisana, J. Rosell, T.K. Mallick, Enhancing performance of a linear dielectric based concentrating photovoltaic system using a reflective film along the edge, Energy 73 (2014) 177–191, http://dx.doi.org/10.1016/j.energy.2014.06.008.

[11] H. Baig, N. Sellami, T.K. Mallick, Performance modeling and testing of a Building Integrated Concentrating Photovoltaic (BICPV) system, Sol. Energy Mater. Sol. Cells 134 (2015) 29–44, http://dx.doi.org/10.1016/j.solmat.2014.11.019.

[12] H. Baig, Enhancing Performance of Building Integrated Concentrating Photovoltaic systems, University of Exeter, 2015, http://hdl.handle.net/10871/17301.

[13] I. Santos-González, M. Sandoval-reyes, O. García-valladares, N. Ortega, Design and evaluation of a compound parabolic concentrator for heat generation of thermal processes, Energy Procedia 57 (2014) 2956–2965, http://dx.doi.org/10.1016/j.egypro.2014.10.331.

[14] K. Shanks, S. Senthilarasu, T.K. Mallick, Optics for concentrating photovoltaics: trends, limits and opportunities for materials and design, Renew. Sustain. Energy Rev. 60 (2016) 394–407, http://dx.doi.org/10.1016/j.rser.2016.01.089.

[15] H.G. Agrell, J. Lindgren, A. Hagfeldt, Degradation mechanisms in a dye-sensitized solar cell studied by UV–VIS and IR spectroscopy, Sol. Energy 75 (2003) 169–180, http://dx.doi.org/10.1016/S0038-092X(03)00248-2.

[16] S.D. Ã, K. Wang, J. Weng, Y. Sui, Y. Huang, S. Xiao, S. Chen, L. Hu, F. Kong, X. Pan, C. Shi, L. Guo, Design of DSC panel with efficiency more than 6 %, Sol. Energy Mater. Sol. Cells 85 (2005) 447–455, http://dx.doi.org/10.1016/j.solmat.2004.10.001.

[17] S. Casaluci, M. Gemmi, V. Pellegrini, A. Di Carlo, F. Bonaccorso, Nanoscale (2016), http://dx.doi.org/10.1039/C5NR07971C.

[18] S. Dai, J. Weng, Y. Sui, C. Shi, Y. Huang, S. Chen, X. Pan, X. Fang, L. Hu, F. Kong, K. Wang, Dye-sensitized solar cells , from cell to module, Sol. Energy Mater. Sol. Cells 84 (2004) 125–133, http://dx.doi.org/10.1016/j.solmat.2004.03.002.

[19] K.J. Moon, S.W. Lee, Y.H. Lee, J.H. Kim, J.Y. Ahn, S.J. Lee, D.W. Lee, S.H. Kim, Effect of TiO2 nanoparticle-accumulated bilayer photoelectrode and condenser lens-assisted solar concentrator on light harvesting in dye-sensitized solar cells, Nanoscale Res. Lett. 8 (2013) 283, http://dx.doi.org/10.1186/1556-276X-8-283.

[20] S. Choi, E. Cho, S. Lee, Y. Kim, D. Lee, Development of a high-efficiency laminated dye-sensitized solar cell with a condenser lens, Opt. Express 19 (Suppl. 4) (2011) A818–A823, http://dx.doi.org/10.1364/OE.19.00A818.

[21] G.D. Barber, P.G. Hoertz, S.H.A. Lee, N.M. Abrams, J. Mikulca, T.E. Mallouk, P. Liska, S.M. Zakeeruddin, M. Grätzel, A. Ho-Baillie, M.A. Green, Utilization of direct and diffuse sunlight in a dye-sensitized solar cell - Silicon photovoltaic hybrid concentrator system, J. Phys. Chem. Lett. 2 (2011) 581–585, http://dx.doi.org/10.1021/jz200112m.

[22] A. Sacco, M. Gerosa, S. Bianco, L. Mercatelli, R. Fontana, L. Pezzati, M. Quaglio, C.F. Pirri, A.O.M. Tucci, Dye-sensitized solar cell for a solar concentrator system, Sol. Energy 125 (2016) 307–313, http://dx.doi.org/10.1016/j.solener.2015.11.026.

[23] V.K. Narra, H. Ullah, V.K. Singh, L. Giribabu, S. Senthilarasu, S.Z. Karazhanov, A.A. Tahir, T.K. Mallick, H.M. Upadhyaya, D – p – A system based on zinc porphyrin dyes for dye-sensitized solar cells : combined experimental and DFT – TDDFT study, Polyhedron 100 (2015) 313–320, http://dx.doi.org/10.1016/j.poly.2015.08.035.

[24] S. Senthilarasu, T.A.N. Peiris, J. Garc, K.G.U. Wijayantha, Preparation of nano-crystalline TiO2 electrodes for flexible dye- sensitized solar cells : influence of mechanical compression, J. Phys. Chem. C (2012).

[25] H. Baig, N. Sellami, T.K. Mallick, Performance modeling and testing of a Building Integrated Concentrating Photovoltaic (BICPV) system, Sol. Energy Mater. Sol. Cells 134 (2015) 29–44, http://dx.doi.org/10.1016/j.solmat.2014.11.019.

[26] S. Yoon, S. Tak, J. Kim, Y. Jun, K. Kang, J. Park, Application of transparent dye-sensitized solar cells to building integrated photovoltaic systems, Build. Environ. 46 (2011) 1899–1904, http://dx.doi.org/10.1016/j.buildenv.2011.03.010.

[27] E. Dissociation, S. States, Q. Yu, Y. Wang, Z. Yi, N. Zu, J. Zhang, M. Zhang, P. Wang, High-efficiency dye-sensitized solar cells: the influence of lithium ions on, 4, n.d., pp. 6032–6038.

[28] M.C. Kao, H.Z. Chen, S.L. Young, C.Y. Kung, C.C. Lin, The effects of the thickness of TiO 2 films on the performance of dye-sensitized solar cells, Thin Solid Films 517 (2009) 5096–5099, http://dx.doi.org/10.1016/j.tsf.2009.03.102.

[29] W. Zhao, H. Bala, J. Chen, Y. Zhao, G. Sun, J. Cao, Z. Zhang, Thickness-dependent electron transport performance of mesoporous TiO2 thin film for dye-sensitized solar cells, Electrochim. Acta 114 (2013) 318–324, http://dx.doi.org/10.1016/j.electacta.2013.09.165.

[30] Q. Wang, J. Moser, M. Gra, Electrochemical impedance spectroscopic analysis of dye-sensitized solar cells, J. Phys. Chem. B (2005) 14945–14953.

[31] E. Section, Determination of the electron lifetime in nanocrystalline dye solar cells by open-circuit voltage decay measurements, ChemPhysChem (2003) 859–864, http://dx.doi.org/10.1002/cphc.200200615.

[32] H. Desilvestro, What physical factors affect current-voltage characteristics of dye solar cells? Dye. Tech. Lit. (2008) 1–16.

[33] K. Okada, H. Matsui, T. Kawashima, T. Ezure, N. Tanabe, 100 mm × 100 mm large-sized dye sensitized solar cells, J. Photochem. Phobiol. A: Chem. 164 (2004) 193–198, http://dx.doi.org/10.1016/j.jphotochem.2004.01.028.

[34] Effect of Light Intensity, n.d. 〈http://www.pveducation.org/pvcdrom/effect-of-light-intensity〉 (Accessed 18 July 2017).

[35] M. Sabry, Temperature optimization of high concentrated active cooled solar cells, NRIAG J. Astron. Geophys. 5 (2016) 23–29, http://dx.doi.org/10.1016/j.nrjag.2016.03.002.

[36] O. Dupré, R. Vaillon, M.A. Green, Thermal behavior of photovoltaic devices, 2017 〈http://dx.doi.org/10.1007/978-3-319-49457-9〉.

[37] P.J. Sebastian, A. Olea, J. Campos, J.A. Toledo, S.A. Gamboa, Temperature dependence and the oscillatory behavior of the opto-electronic properties of a dye-sensitized nanocrystalline TiO2 solar cell, Sol. Energy Mater. Cell 81 (2004) 349–361, http://dx.doi.org/10.1016/j.solmat.2003.11.011.

[38] K.J. Moon, S.W. Lee, Y.H. Lee, J.H. Kim, J.Y. Ahn, S.J. Lee, D.W. Lee, S.H. Kim, Effect of TiO2 nanoparticle-accumulated bilayer photoelectrode and condenser lens-assisted solar concentrator on light harvesting in dye-sensitized solar cells, Nanoscale Res. Lett. 8 (2013) 283, http://dx.doi.org/10.1186/1556-276X-8-283.